The Use of Volume-Averaging Techniques to Predict Temperature Transients Due to Water Vapor Sorption in Hygroscopic Porous Polymer Materials

PHILLIP GIBSON[1] **MAJID CHARMCHI**[2]

[1] U.S. Army Natick Research, Development and Engineering Center, Natick, Massachusetts 01760-5019

[2] Department of Mechanical Engineering, University of Massachusetts Lowell, Lowell, Massachusetts 01854

Received 15 July 1996; accepted 7 September 1996

ABSTRACT: Volume-averaging techniques developed for modeling drying processes in porous materials offer a convenient framework for analyzing vapor sorption in porous hygroscopic polymeric materials. Because of the large temperature changes associated with water vapor sorption in these materials (from 10° to 20°C), sorption/diffusion processes are best characterized through the coupled differential equations describing both the transport of energy and mass through the porous structure. Experimental and numerical results are compared for a variety of natural and man-made porous polymeric materials (textiles) using the volume-averaging technique. Boundary heat and mass transfer coefficients and assumptions about thermal radiative properties of the experimental apparatus are shown to influence results obtained with the numerical solution method. © 1997 John Wiley & Sons, Inc. *J Appl Polym Sci **64:** 493–505, 1997

Key words: diffusion; sorption; water vapor; porous materials; textiles

INTRODUCTION

Accurate models for the coupled diffusion of heat and vapor through porous polymeric materials (fabrics, foams, particle beds, etc.) are of technological importance for applications such as filtration media, clothing systems, textile preforms for composites, and industrial processes involved in manufacturing textiles and textile-based commodities. The one-dimensional case of transient diffusion in hygroscopic porous textiles is convenient for illustrating the use of volume-averaging techniques which aid in the numerical solution of partial differential equations which describe coupled diffusion processes in these materials.

Fundamental studies by Henry[1] on how the sorptive properties of wool fibers produce a buffering effect between the human body and the ambient environment were incorporated by Crank[2] in his classic work on the mathematics of diffusion. The heat released as water vapor diffuses through, and is absorbed by, a bed of hygroscopic fibers; and this is significant for processing operations, such as when bales of wool or cotton must be dried to a specified moisture content. Similarly, for woolen clothing, the heat released or absorbed when the relative humidity or temperature within a woolen textile layer changes is often physiologically significant. Various workers have extended Henry's approach over the years, most notably Nordon and David[3]; Farnworth[4]; Wehner, Miller, and Rebenfeld[5]; Jones, Ito, and McCullough[6]; Li and Holcombe[7]; and Le and Ly.[8] While continuing to concentrate on the coupled diffusion processes for energy and water vapor through porous hygro-

Correspondence to: Phillip Gibson.

 CCC 0021-8995/97/030493-13

scopic layers, each group made different assumptions concerning the nature of the sorption process within the hygroscopic fiber.

The groups mentioned above all focused on woven and nonwoven textiles as the materials of interest. A great many more studies have been undertaken for the coupled heat and mass-transfer problem through porous media in general. Much of the literature on the drying of capillary porous bodies or hygroscopic porous materials is directly applicable to the problem of mass and energy transport through textile materials. Many studies concentrate on a limited set of materials, derive a small number of partial differential equations based on either diffusion or convection, and develop solutions based on these particular situations. Well-known examples of this approach include studies by Berger and Pei,[9] Eckert and Faghri,[10] and Stanish et al.[11] More comprehensive systems of equations which account for diffusion of heat and water vapor, along with convective gas flows and capillary liquid transport, are available in works by Luikov[12] and Whitaker.[13] The approach taken by Whitaker, in particular, has been adopted by many groups investigating transfer of heat and moisture through food materials (drying) and thermal insulation. Tao, Besant, and Rezkallah[14] successfully applied Whitaker's approach to a fibrous insulation which releases heat due to sorption of water vapor by a hygroscopic resin on a nonhygroscopic fiber and also due to condensation occurring within the porous structure. They showed that the transient nature of the heat flow process in fibrous materials can produce large errors if the heat of sorption is ignored in an analysis.

In this paper, we apply these general volume-averaging techniques to the prediction of the transient temperature changes and equilibration times of hygroscopic materials used in clothing systems. The one-dimensional model described here has proven to be useful in more general models which couple the transient thermal behavior of clothing systems to models of the human thermoregulatory system,[15,16,17] making it possible to incorporate time-dependent transport and sorption properties of clothing materials into the evaluation of new protective clothing candidates.

GOVERNING DIFFERENTIAL EQUATIONS

A set of equations which describe the transient diffusion of heat and mass through hygroscopic porous materials is summarized in this section. The equations derive from the general governing equations given by Gibson,[18] which were obtained by volume-averaging techniques using definitions for intrinsic phase average, phase average, and spatial average for porous media given by Whitaker.[13] The general equations include liquid transport and accumulation, as well as convective gas flow effects, which are not included in the coupled-diffusion examples given in this paper.

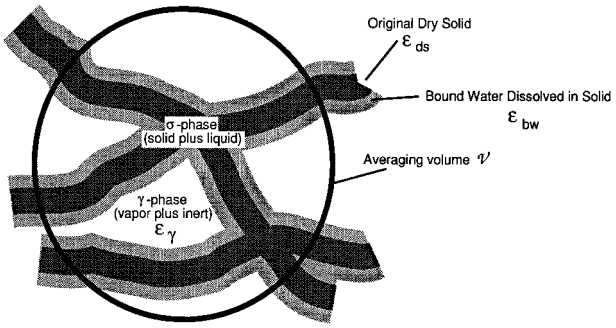

Figure 1 Schematic for definition of "bound water" volume fraction ε_{bw}.

We define the "solid phase" as the polymer volume fraction plus the volume of the "bound water" which is dissolved in the solid phase. An illustration of the bound water volume fraction is shown in Figure 1.

In this particular set of equations, the major simplifying assumptions are: (1) there is no liquid or gas phase convection, (2) there is no liquid phase present, (3) the volume of the solid phase is equal to the volume of the dry solid polymer plus the volume of the bound water, (4) mass transport predominately occurs through the gas phase, and (5) the transport is one-dimensional (x-direction). Definitions for the symbols used are given in the Nomenclature section.

Energy equation:

$$\rho C_p \frac{\partial T}{\partial t} + (Q_l + \Delta h_{\text{vap}})\dot{m}_{sv} = \frac{\partial}{\partial x}\left(k_{\text{eff}} \frac{\partial T}{\partial x}\right) \quad (1)$$

Solid phase continuity equation:

$$\rho_w \frac{\partial}{\partial t}(\varepsilon_{bw}) + \dot{m}_{sv} = 0 \quad \text{or}$$

$$\frac{\partial}{\partial t}(\varepsilon_{bw}) + \frac{\dot{m}_{sv}}{\rho_w} = 0 \quad (2)$$

Gas phase diffusion equation:

$$\frac{\partial}{\partial t}(\varepsilon_{\gamma}\rho_v) - \dot{m}_{sv} = \frac{\partial}{\partial x}\left(\mathcal{D}_{\text{eff}} \frac{\partial \rho_v}{\partial x}\right) \quad (3)$$

Volume fraction constraint:

$$\varepsilon_\gamma + \varepsilon_{bw} + \varepsilon_{ds} = 1 \quad (4)$$

Thermodynamic relations:

$$p_a = p_\gamma - p_v \quad (5)$$

$$p_a = \rho_a \frac{R}{M_a} T \quad (6)$$

$$p_v = \rho_v \frac{R}{M_w} T \quad (7)$$

Sorption relation[19]:

$$\varepsilon_{bw} = 0.578 R_f \left(\varepsilon_{ds} \frac{\rho_{ds}}{\rho_w} \right) (\phi) \times \left[\frac{1}{(0.321 + \phi)} + \frac{1}{(1.262 - \phi)} \right] \quad (8)$$

The source term due to vapor sorption is modeled by assuming that diffusion into the fiber is quasisteady state.[7] The polymer at the fiber's surface is assumed to immediately come into equilibrium with the relative humidity of the gas phase within the control volume for that grid point. The mass flux into or out of the fiber is calculated by:

$$\dot{m}_{sv} = \frac{D_{\text{solid}} \rho_{ds}}{d_f^2} (R_{\text{total}} - R_{\text{skin}}) \quad (9)$$

where R_{total} is the instantaneous fiber regain (kg of water/100 kg of dry polymer) (fraction); R_{skin} is the equilibrium regain at relative humidity within the control volume (fraction); D_{solid} is the apparent solid phase diffusion coefficient (m^2; and d_f is the apparent fiber diameter (m).

Transport Coefficients and Mixture Properties

For fabrics with significant porosity, an expression for the effective thermal conductivity is given by[20,21]:

$$k_{\text{eff}} = k_\gamma \left\{ \frac{[1 + (\varepsilon_{bw} + \varepsilon_{ds})] k_\sigma + \varepsilon_\gamma k_\gamma}{\varepsilon_\gamma k_\sigma + [1 + (\varepsilon_{bw} + \varepsilon_{ds})] k_\gamma} \right\} \quad (10)$$

$$k_\gamma = \left(\frac{k_v \rho_v + k_a \rho_a}{\rho_v + \rho_a} \right) \quad (11)$$

$$k_\sigma = \left(\frac{k_w \rho_w \varepsilon_{bw} + k_{ds} \rho_{ds} \varepsilon_{ds}}{\rho_w \varepsilon_{bw} + \rho_{ds} \varepsilon_{ds}} \right) \quad (12)$$

$$\mathcal{D}_{\text{eff}} = \frac{\mathcal{D}_a \varepsilon_\gamma}{\tau} \quad (13)$$

$$\mathcal{D}_a (\text{m}^2 \cdot \text{s}^{-1}) = 2.23 \times 10^{-5} \left(\frac{T}{273.15} \right)^{1.75} \quad (14)$$

$$Q_l (\text{J/kg}) = 1.95 \times 10^5 (1 - \phi) \times \left[\frac{1}{(0.2 + \phi)} + \frac{1}{(1.05 - \phi)} \right] \quad (15)$$

$$\Delta h_{\text{vap}} (\text{J/kg}) = 2.792 \times 10^6 - 160T - 3.43T^2 \quad (16)$$

$$p_s (\text{N} \cdot \text{m}^{-2}) = 614.3 \exp \left\{ 17.06 \left[\frac{(T - 273.15)}{(T - 40.25)} \right] \right\} \quad (17)$$

Initial and Boundary Conditions

Initial conditions are: $T(x, t = 0) = T_0$; $\rho_v(x, t = 0) = \phi_0 p_s(@T_0)$; and $\varepsilon_{bw}(x, t = 0) = \varepsilon_{bw0}$. Boundary conditions ($L$ refers to fabric thickness are:

$$h_c (T_\infty - T)_{x=0} = -k_{\text{eff}} \frac{\partial T}{\partial x} \Big]_{x=0} = h_c (T_\infty - T)_{x=L} = -k_{\text{eff}} \frac{\partial T}{\partial x} \Big]_{x=L} \quad (18)$$

$$h_m (\rho_{v\infty} - \rho_v)_{x=0} = -D_{\text{eff}} \frac{\partial \rho_v}{\partial x} \Big]_{x=0} = h_m (\rho_{v\infty} - \rho_v)_{x=L} = -\text{D}_{\text{eff}} \frac{\partial \rho_v}{\partial x} \Big]_{x=L} \quad (19)$$

EXPERIMENTAL

We selected seven different types of hygroscopic porous textile materials to evaluate for transport properties. These materials spanned a range of fiber types and constructions and varied in their physical properties (such as thickness) and water vapor sorption properties. The materials' physical properties[22,23] are shown in Table I. For materials

Table I Test Material Physical Properties

Material	Thickness (m)	Dry Solid Density (kg/m^3) (ρ_{ds})	Dry Solid Volume Fraction (ε_{ds})	Regain (@ $\phi = 0.65$) (R_f)	Heat Capacity [J/(kg·K)] [$(c_p)_{ds}$]	Thermal Conductivity [J/(s·m·K)] (k_{ds})
Wool	6.43×10^{-4}	1300	0.381	0.150	1360	0.20[a]
Silk	1.35×10^{-4}	1340	0.361	0.100	1380	0.20[a]
Cotton	3.84×10^{-4}	1550	0.336	0.070	1210	0.16
Wool/Polyester	4.42×10^{-4}	1354	0.384	0.062	1348	0.16
Nylon/Cotton	4.63×10^{-4}	1345	0.409	0.056	1320	0.20
Nylon	8.61×10^{-4}	1140	0.360	0.041	1430	0.25
Polyester	5.89×10^{-4}	1390	0.293	0.004	1340	0.14

[a] estimated.

which were a mixture of two or more materials, we used a mass fraction-weighted average of individual component properties.

Experimental data were collected with an apparatus which is capable of evaluating the transport properties of textiles under conditions of pure diffusion (concentration gradient), combined diffusion/convection (concentration and pressure gradients), and pure convection (pressure gradients only). A schematic of the test device, which we call the Dynamic Moisture Permeation Cell (DMPC), is shown in Figure 2.

The DMPC is normally used to obtain steady-state diffusion properties[24] or steady-state diffusion/convection properties.[25] The DMPC may also be used to obtain records of temperature transients due to water vapor sorption for materials subjected to step changes in relative humidity. The rate at which the temperature rises and falls is related to the mass transport and thermal transport properties of the test sample and serves as a convenient experimental verification of the numerical prediction of transient behavior. In these experiments, thermocouples were sandwiched between two layers of material to record temperature changes as the test sample absorbed or desorbed water vapor from the gas stream flowing on the two sides of the DMPC. Three thermocouples were used as shown in Figure 3. The thermocouple diameter was 1.27×10^{-4} m (0.005 inch), with a response time listed by the manufacturer as 0.04 s in water and 1 s in still air. Smaller thermocouples with a diameter of 2.54×10^{-5} m (0.001 inch) were used initially but proved to be quite fragile and easily damaged. The temperature changes recorded with both sizes of thermocouples were identical, so we believe that errors due to conduction and the heat capacity of the thermocouple wires are minimal.

An example of the temperature transients for all seven test materials, for a step change from 0.0 to 1.0 relative humidity, is shown in Figure 4. Here only the first three minutes are shown, to make it easier to distinguish the response of the different materials shown. The peak temperature for each material is also shown on the plot.

Figure 4 can be misleading, in that it shows a single well-defined experimental temperature transient for each material. There are concentration and temperature gradients down the length of the test sample; and, due to the influence of the developing thermal and concentration boundary layers, the temperatures of the upstream, center, and downstream thermocouples (refer to Figure 3) are slightly different, as shown in Figure 5.

There is also significant variability in the temperature traces obtained for different pieces of the same fabric at different times. Figure 6 shows various results obtained for different samples of the cotton fabric, again for water vapor sorption, under a step change in relative humidity from 0.0 to 1.0, at 20°C.

Another transient measurement, which is useful for verifying numerical predictions of transient diffusion behavior, is the experimental measurement of the water vapor concentration change on one side of the sample as the relative humidity on the other side of the sample is changed. Following a step change in relative humidity, the rate of change of the measured relative humidity on the "dry side" of the cell is greatly affected by the sorption kinetics of a hygroscopic material. Figure 7 shows the change in relative humidity on one side of the DMPC when the humidity on the other

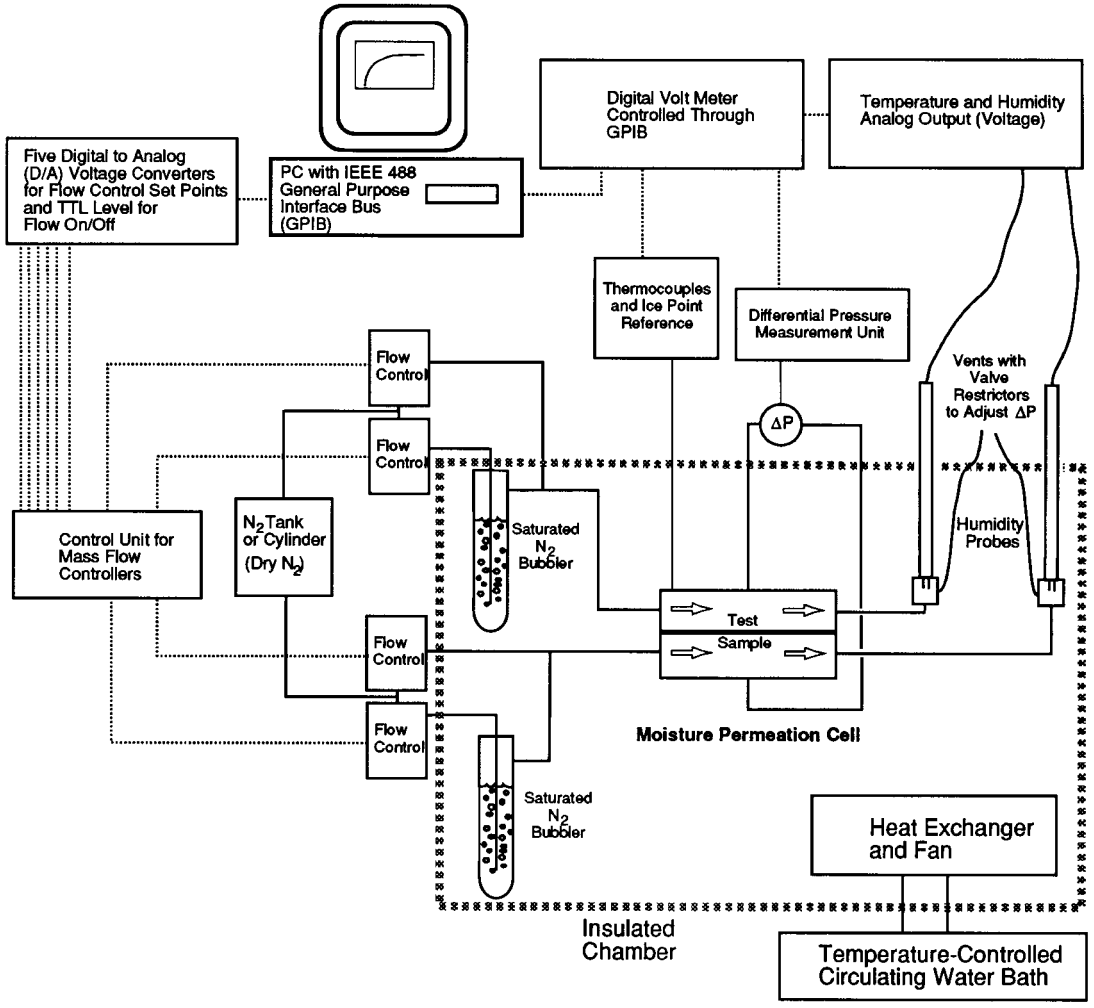

Figure 2 Schematic of DMPC test arrangement.

side is suddenly changed to 0.6. Figure 7 has had the relative humidity normalized by the final equilibrium relative humidity. Also shown in Figure 7 are the results for two layers of a microporous polytetrafluoretheylene membrane, which is completely nonhygroscopic and has a very low resistance to vapor diffusion and which serves to indicate the response time of the relative humidity sensors to a step change in humidity.

To proceed to a numerical solution of the coupled-diffusion problem for these materials, we also require numerical values for the external convective heat and mass transfer coefficients at the boundaries of the test sample. The external convective mass transfer coefficient h_m is available from measurements in the DMPC. For the particular flow rates and temperature used in the steady-state diffusion experiments, the apparent boundary layer resistance is typically about 95 s/m.[24] Assuming that the boundary layers are equal on the two sides of the sample, each side had a resistance of 47.5 s/m, which results in a mass transfer coefficient h_m of 0.021 m/s.

An estimate of the external convective heat transfer coefficient may be found from boundary layer similarity[26] (assuming laminar flow):

$$h_c = h_m[\rho_\gamma (c_p)_a] \left(\frac{\alpha}{D_a}\right)^{2/3} \qquad (20)$$

where α = thermal diffusivity of gas (m^2/s); D_a = diffusion coefficient of water vapor in air (m^2/s); ρ_γ = gas density; and $(c_p)_a$ = gas heat capacity. This results in an external convective heat transfer coefficient of $h_c = 21.8$ W/($m^2 \cdot s$).

However, we may also estimate convective heat transfer coefficients using relations developed for

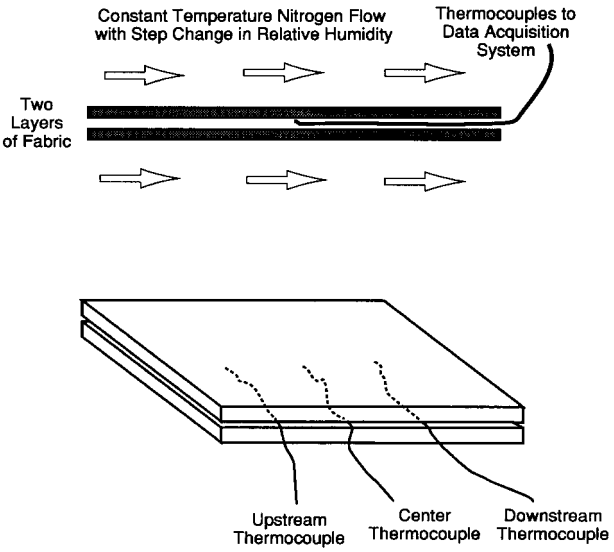

Figure 3 Instrumented test fabric in DMPC to record temperature changes of hygroscopic materials.

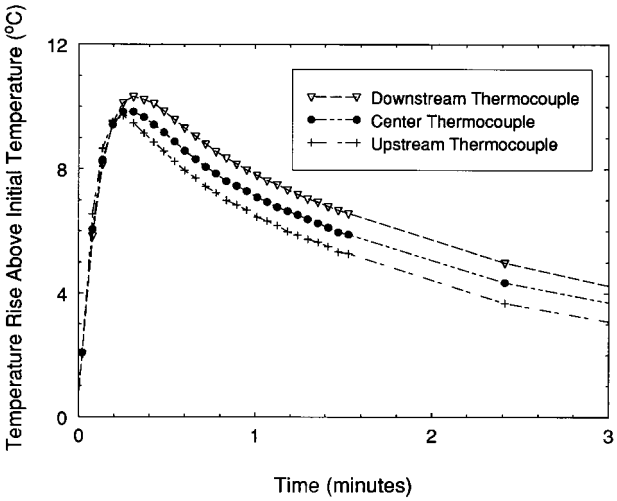

Figure 5 Temperature changes for the three thermocouples for the cotton fabric, due to water vapor sorption during step change in relative humidity from 0.0 to 1.0.

flow between parallel plates.[27] Using these relations, we get a heat transfer coefficient of around 40 $W/(m^2 \cdot s)$. Since the thermal boundary layer over the test sample is not fully developed, the assumptions about boundary layer similarity may not be justified, and the heat transfer coefficient for flow between parallel plates can be used. Later in this paper we compare results obtained using these two different heat transfer coefficients, and we also include simple thermal radiation effects.

This problem of uncertainty about what boundary heat transfer coefficients to use in our numerical solution does not arise if one models the full flow field in the DMPC,[25] since the flow simulation will take care of all the momentum, concentration, and temperature boundary layers in the course of the fluid dynamic and heat/mass transfer calculations for the flowing gas streams.

The steady-state diffusion properties of the experimental samples, measured with the DMPC, are given in Table II. Also given in Table II are the assumed properties of effective fiber diameter d_{eff} and effective solid phase diffusion coefficient

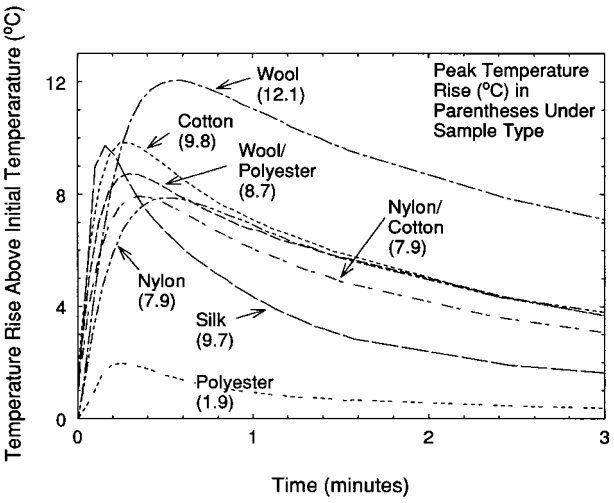

Figure 4 Temperature changes due to water vapor sorption for seven fabrics during step change in relative humidity from 0.0 to 1.0.

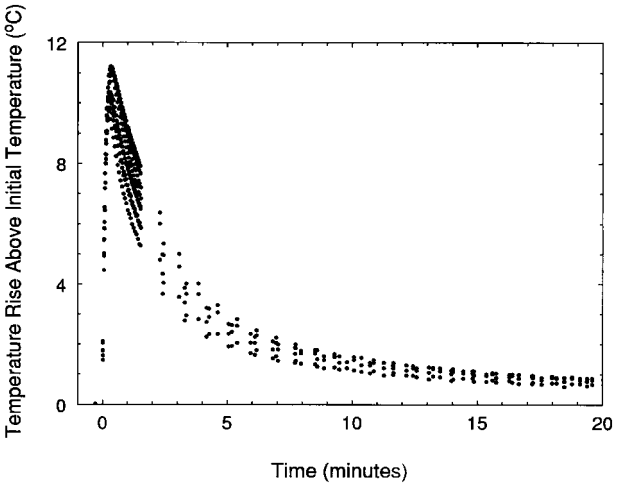

Figure 6 Variability in measured temperature changes for the cotton fabric, due to water vapor sorption during step change in relative humidity from 0.0 to 1.0.

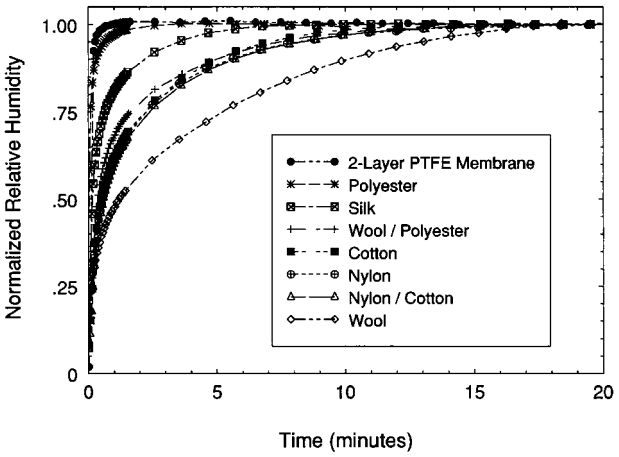

Figure 7 Relative humidity normalized by final equilibrium value, during step change from 0.0 to 0.6, at constant temperature of 20°C.

D_{solid} which take care of the actual geometry of the fiber, including fiber/yarn shape and fiber/yarn size distribution, both chosen to fit the transient experimental data.

COMPARISON OF EXPERIMENTAL AND NUMERICAL RESULTS

A one-dimensional numerical code, based on a finite-difference control-volume approach,[28] was used to solve the system of equations. The situation modeled was the step change in relative humidity from 0.0 to 1.0 at a temperature of 20°C. Typical experimental results were shown in Figure 4, and the experimental schematic was shown previously in Figure 3.

Figures 8 and 9 show the comparison of the computed and the experimental temperature history as a function of time, for the seven fabrics. The experimental data contain more data points in the first minute to resolve the initial fast temperature changes.

We see fairly good agreement between measured and predicted temperature transients for all the fabrics. The comparisons shown are for the center thermocouple only and are thus average values. There is actually a significant temperature and concentration variation down the length of the sample in the DMPC apparatus during the vapor sorption process which is reflected in the different temperature records from the three thermocouples in the test sample.

The one-dimensional numerical model may also be used to examine features of hygroscopic porous materials such as equilibration time and weight change due to vapor uptake. This is convenient when data from an apparatus such as a sorption balance are available.

Figure 10 shows the performance of the one-dimensional model for the sorption of water vapor, following a step change from 0.0 to 0.65 relative humidity, at 20°C, under the same conditions as given before for the DMPC, for the seven fabrics in Table II. The results plot the fractional approach to equilibrium regain at 65% relative humidity.

Figure 10 agrees with the trends shown in Figure 7, which also shows the fractional approach to equilibrium of the seven fabrics, although under conditions of a humidity gradient across the sample. In both cases, the wool fabric is the slowest to equilibrate; the group of four fabrics (cotton, nylon/cotton, nylon, and wool/polyester) are very similar in their times to equilibrate; and the silk fabric is intermediate between this group and the polyester fabric, which equilibrates the fastest.

Table II Test Fabric Transport Properties

Material	Diffusion Properties: D_{eff} (Fabric Diffusivity) (m^2/s)	Diffusion Properties: τ (Tortuosity Factor)	Sorption Rate Factor (D_{solid}/d_f^2) (s^{-1})
Wool	6.63×10^{-6}	2.35	2.31×10^{-2}
Silk	4.09×10^{-6}	3.94	9.06×10^{-2}
Cotton	7.60×10^{-6}	2.12	3.44×10^{-2}
Wool/Polyester	7.24×10^{-6}	2.14	3.19×10^{-2}
Nylon/Cotton	5.97×10^{-6}	2.49	2.69×10^{-2}
Nylon	8.87×10^{-6}	1.82	4.81×10^{-2}
Polyester	1.19×10^{-5}	1.50	4.89×10^{-2}

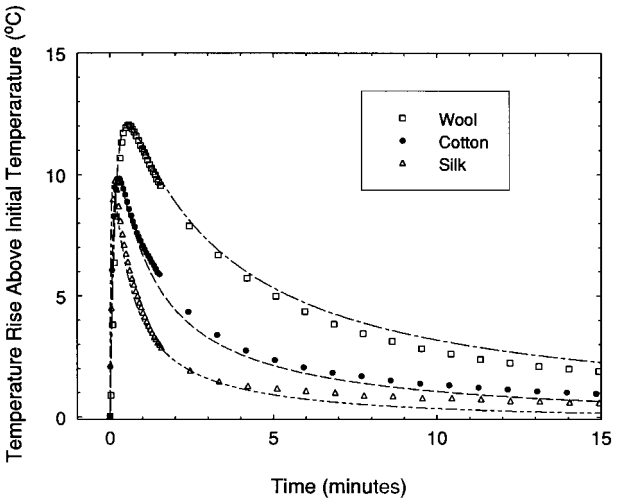

Figure 8 Comparison of numerical predictions to experimental results of centerline temperature of wool, cotton, and silk fabrics subjected to step change in relative humidity.

THERMAL HYSTERESIS OF HYGROSCOPIC MATERIALS DUE TO VAPOR SORPTION

One of the reasons that hygroscopic fibers such as cotton and wool are thought to be more comfortable is that they have the ability to buffer concentration or temperature changes occurring between the environment and the human body. This effect is best examined using models which couple transient clothing behavior to human thermoregulatory models,[15,16,17] but it is instructive to use the one-dimensional model to observe the effects of a sudden change in temperature on one side of a fabric barrier.

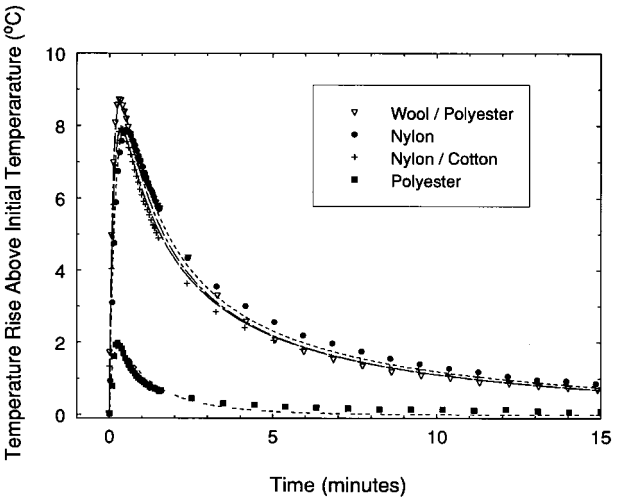

Figure 9 Comparison of numerical predictions to experimental results of centerline temperature of wool/polyester, nylon/cotton, nylon, and polyester fabrics subjected to step change in relative humidity.

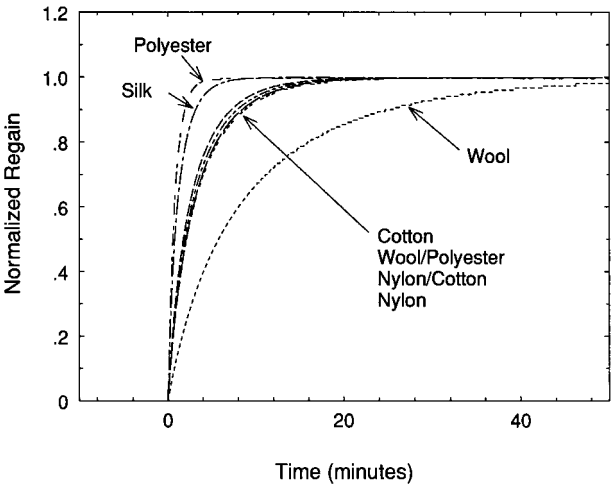

Figure 10 Fractional approach to equilibrium at 65% relative humidity and 20°C, for seven materials.

A practical example often cited in the literature is that of a material such as a wool fabric which is used for cool weather clothing. If a person wearing a wool coat inside a building where it is warm and dry then goes outside to a colder environment, which may have a higher humidity, the wool coat will buffer the temperature change due to the tendency of the wool fibers to absorb water vapor from the air and release the heat of sorption. These types of effects may also be important in applications such as building insulation, where even though fiberglass itself is not very hygroscopic, the resinous binders used to stabilize the batts have an affinity for water and may cause significant temperature transients due to absorption processes.[14]

We can use our one-dimensional numerical model to examine this thermal hysteresis effect for a typical hygroscopic textile. The material properties are those of two layers of the wool fabric given in Tables I and II. The fabric is first equilibrated at 30°C and 0.40 relative humidity. The ambient temperature and ambient relative humidity on one side of the fabric are then suddenly changed to 5°C and 0.90, as shown in Figure 11. The external heat and mass transfer coefficients on both sides of the fabric are kept the same as those used in the previous simulations.

We examine the performance of the one-dimensional model for two cases. In Case I, we turn off the hygroscopic character of the fibers by setting the fabric regain to zero. In Case II, we turn the

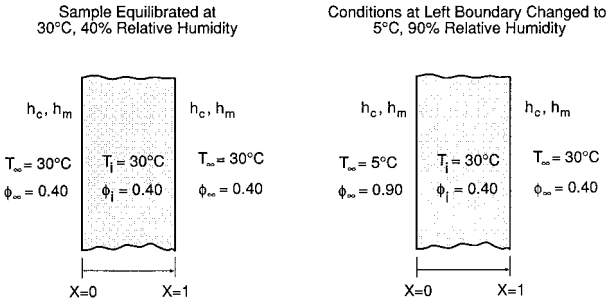

Figure 11 Numerical experiment to simulate sudden temperature and relative humidity change on one side of a fabric.

normal hygroscopic character of the wool fibers back on using the proper value for the regain of wool. All the other properties of the fabric remain the same, and we can observe the consequences of vapor sorption as unaffected by any other physical properties (although we should mention that the thermal conductivity and heat capacity of the hygroscopic fabric change slightly over time as the fabric's proportion of bound water increases).

In Figure 12, we see the expected behavior of a hygroscopic fabric as compared to a nonhygroscopic fabric. For Case I, the nonhygroscopic fabric, the material equilibrates very quickly; and the temperature of the center of the fabric quickly assumes the mean temperature of the two sides (17.5°C), valid for steady-state conduction with constant heat capacity and thermal conductivity. For Case II, the hygroscopic fabric, significant vapor sorption takes place which serves an energy source within the fabric. The equilibration time

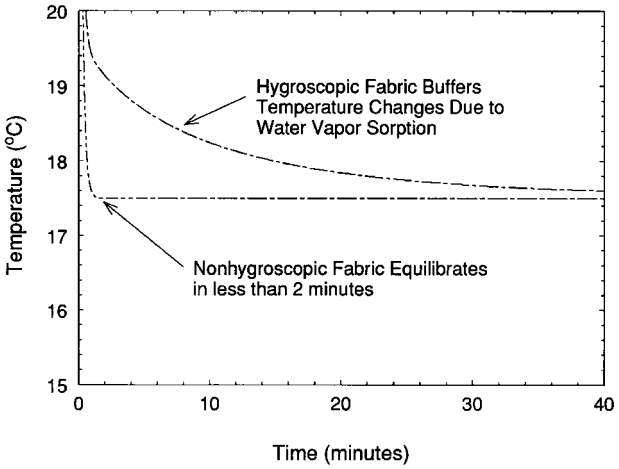

Figure 12 Change in centerline temperature of a hygroscopic and a nonhygroscopic fabric as the ambient conditions are changed on one side.

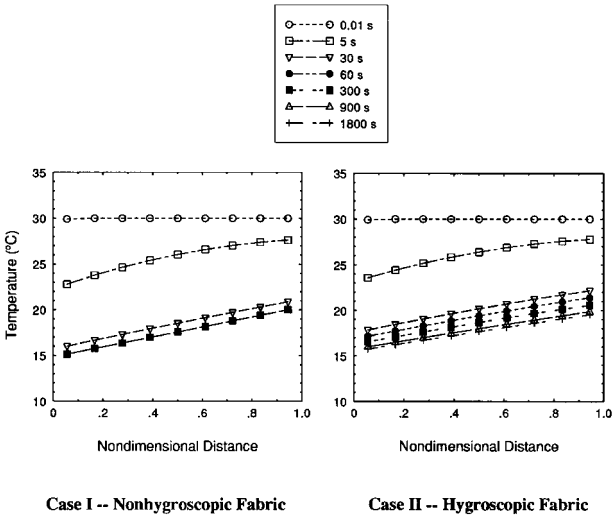

Figure 13 Calculated temperature profiles through the nonhygroscopic and the hygroscopic fabric at various times after ambient conditions on one side are changed.

is thus much longer: 30 min for the hygroscopic fabric, versus 2 min for the nonhygroscopic fabric.

The numerical solution also makes it possible to show the calculated temperature profiles through the thickness of the material at different times, after the ambient temperature and humidity are changed on one side of the fabric (Figure 13).

In a similar manner, we may also examine the gas-phase water vapor concentration profile within the fabric. Figure 14 shows the calculated

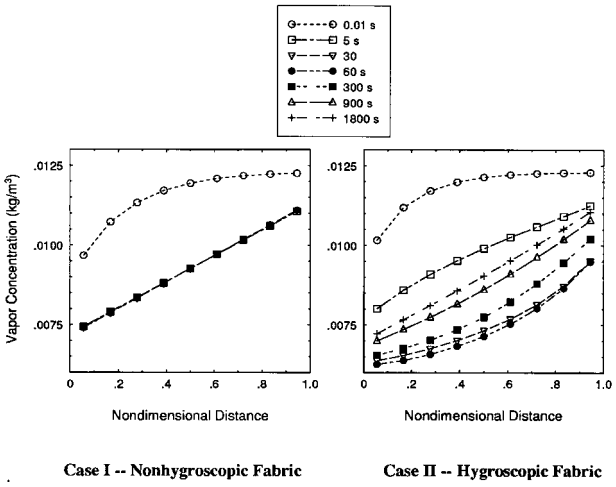

Figure 14 Calculated water vapor concentration profiles through the nonhygroscopic and the hygroscopic fabric at various times after conditions on one side are changed.

water vapor concentration through the fabric thickness, for the hygroscopic and nonhygroscopic fabrics as a function of time. Vapor concentration is chosen rather than relative humidity, since the saturation vapor pressure is a function of temperature and relative humidity can be confusing when temperature gradients are involved.

Figure 14 shows that the nonhygroscopic fabric equilibrates within a matter of seconds, but that the hygroscopic wool fabric takes much longer because of the sorption kinetics of the fibers as they come to equilibrium with the local water vapor concentration in the fabric pores and also because of the value of the local temperature which affects the gas phase partial vapor pressures.

EFFECT OF DIFFERENT BOUNDARY HEAT TRANSFER COEFFICIENTS ON NUMERICAL RESULTS

We have noted that we had to assume a heat transfer coefficient, and we could choose values that ranged from about 20 to 40 W/($m^2 \cdot s$). We may use the one-dimensional numerical code to examine the consequences of using various assumptions about the boundary heat-transfer coefficients. In addition to varying the convective heat transfer coefficient, we may also include an effective radiative heat transfer coefficient and examine the potential importance of thermal radiation heat losses on the calculated temperature transients.

The simplest thermal radiation heat transfer coefficient may be defined as that between two parallel plates at different temperatures.[29] An effective heat-transfer coefficient is defined as the sum of the convective heat-transfer coefficient (h_c) and a thermal radiative heat-transfer coefficient (h_r):

$$h_{\text{eff}} = (h_c + h_r) \tag{21}$$

We will assume that the emissivity of the fabric and the plastic duct are both equal to 0.9, which allows the thermal radiative heat transfer coefficient to be written as:

$$h_r = \varepsilon\sigma(T_f + T_w)(T_f^2 - T_w^2) \tag{22}$$

where: ε = emissivity (assumed to be 0.9); σ = Stefan Boltzmann constant [5.669×10^{-8} W/($m^2 \cdot K^4$)]; T_f = fabric temperature (K); and T_w = duct wall temperature (K).

Figure 15 shows the effects of three different boundary heat transfer coefficients on the calculated temperature transients for the cotton fabric, with the sorption rate factor adjusted to give equal peak temperatures which match the experimental results. There are some differences among the different assumptions; but, referring back to the experimental data scatter contained in Figure 6, the differences are fairly minor.

Figure 16 shows how the different heat transfer coefficient assumptions affect the rate at which the cotton fabric approaches sorptive equilibrium. In this case, the differences are due more to the

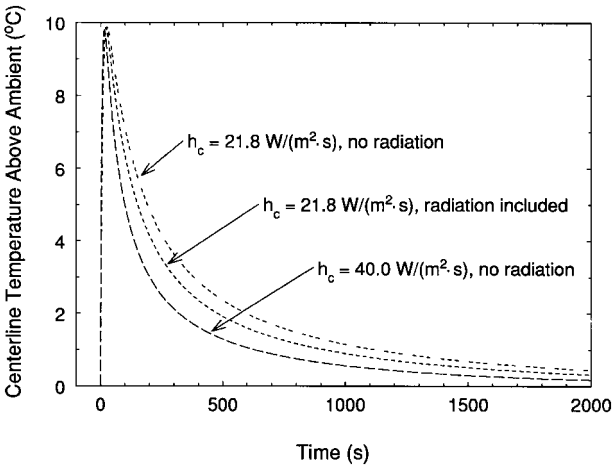

Figure 15 Effect of different boundary heat transfer coefficients on calculation of temperature transients during water vapor sorption for a cotton fabric.

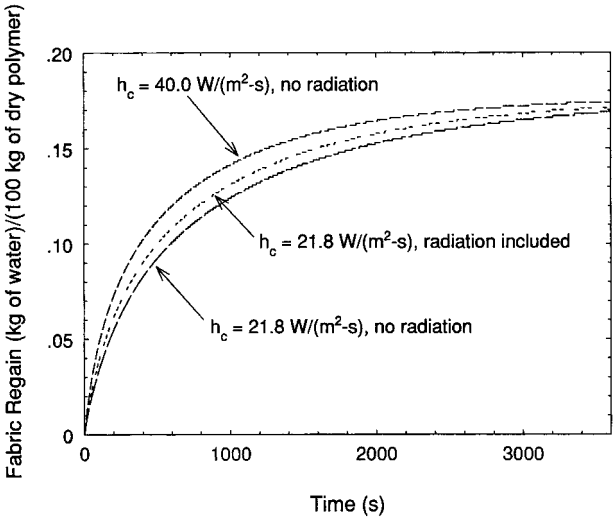

Figure 16 Effect of different boundary heat transfer coefficients on water vapor sorption for a cotton fabric.

different sorption rate factors, rather than to a direct influence of the boundary heat transfer coefficient.

CONCLUSIONS

The one-dimensional model of coupled diffusion of mass and energy in hygroscopic porous materials performs well in predicting and simulating temperature changes as a function of time and weight changes as a function of time—two quantities that are easily measured experimentally. The use of volume-averaging techniques allows a consistent general treatment of the effects associated with the interactions between the solid and the gas phase during diffusion through porous media. However, the one-dimensional model neglects factors such as the convective transfer of energy and mass through the porous structure of textiles, which can often be of more practical significance than the diffusion properties. The one-dimensional model also neglects radiative transfer, although this can be incorporated in a fairly simple fashion by an effective thermal conductivity which accounts for radiative transfer.

NOMENCLATURE

c_p constant pressure heat capacity [J/(kg·K)]
$(c_p)_{ds}$ constant pressure heat capacity of the dry solid [J/(kg·K)]
$(c_p)_w$ constant pressure heat capacity of liquid water [4182 J/(kg·K) @290 K]
$(c_p)_v$ constant pressure heat capacity of water vapor [1862 J/(kg·K) @290 K]
$(c_p)_a$ constant pressure heat capacity of dry air [1003 J/(kg·K) @290 K]
C_p mass fraction weighted average constant pressure heat capacity [J/(kg·K)]
d_f effective fiber diameter (m)
D_a diffusion coefficient of water vapor in air (m^2/s)
D_{eff} effective gas phase diffusivity (m^2/s)
D_{solid} effective solid phase diffusion coefficient (m^2/s)
Δh_{vap} enthalpy of vaporization per unit mass (J/kg)
h_c convective heat transfer coefficient at boundary [W/(m^2·s)]
h_{eff} effective heat transfer coefficient ($h_c + h_r$) at boundary [W/(m^2·s)]
h_m convective mass transfer coefficient at boundary [W/(m^2·s)]
h_r radiation heat transfer coefficient at boundary [W/(m^2·s)]
k_{ds} thermal conductivity of the dry solid [J/(s·m·K)]
k_{eff} effective thermal conductivity of the porous material [J/(s·m·K)]
k_w thermal conductivity of liquid water [0.600 J/(s·m·K) @290 K]
k_v thermal conductivity of saturated water vapor [0.0246 J/(s·m·K) @380 K]
k_a thermal conductivity of dry air [0.02563 J/(s·m·K) @290 K]
$\dot{m}_{sv}$ mass rate of desorption from solid phase to vapor phase per unit volume [kg/(s·m^3)]
M_a molecular weight of air (28.97 kg/kg mol)
M_w molecular weight of water vapor (18.015 kg/kg mol)
p pressure (N/m^2)
p_γ total gas pressure (N/m^2)
p_a partial pressure of air (N/m^2)
p_v partial pressure of water vapor (N/m^2)
p_s saturation vapor pressure (function of T only) (N/m^2)
Q_1 differential enthalpy of desorption from solid phase to liquid phase per unit mass (J/kg)
R universal gas constant [8314.5 N·m/(kg·K)]
R_f textile measurement (@$\phi = 0.65$), grams of water absorbed per 100 grams of fiber (fraction)
R_{skin} equilibrium regain at fiber surface (fraction)
R_{total} total fiber regain from last time step (fraction)
T temperature (K)
t time (s)
$V_{bw}(t)$ volume of the bound water contained within the averaging volume (m^3)
$V_\sigma(t)$ volume of the solid phase contained within the averaging volume (m^3)
$V_\beta(t)$ volume of the liquid phase contained within the averaging volume (m^3)
$V_\gamma(t)$ volume of the gas phase contained within the averaging volume (m^3)
$\mathcal{V}$ averaging volume (m^3)

Greek Letters

$\varepsilon_\sigma(t)$	$V_\sigma/\mathcal{V}$, volume fraction of the solid phase
$\varepsilon_\beta(t)$	$V_\beta/\mathcal{V}$, volume fraction of the liquid phase
$\varepsilon_\gamma(t)$	$V_\gamma/\mathcal{V}$, volume fraction of the gas phase
ε_{ds}	$V_{ds}/\mathcal{V}$, volume fraction of the dry solid (constant)
$\varepsilon_{bw}(t)$	$V_{bw}/\mathcal{V}$, volume fraction of the water dissolved in the solid phase
$\varepsilon_{\text{bwsat}}$	volume fraction of bound water at ϕ = 1.0
ϕ	p_v/p_s, relative humidity
ρ	volume average density of the porous material (kg/m^3)
ρ_{ds}	density of dry solid (for polymers typically 900 to 1300 kg/m^3)
ρ_w	density of liquid water (approximately 1000 kg/m^3)
ρ_γ	density of gas phase (mixture of air and water vapor) (kg/m^3)
ρ_v	density of water vapor in the gas volume (equivalent to mass concentration) (kg/m^3)
ρ_a	density of the inert air component in the gas volume (equivalent to mass of air/total gas volume) (kg/m^3)
τ	tortuosity factor

Subscripts

0	initial
∞	free stream
l	liquid
s	solid
σ	designates a property of the solid phase
β	designates a property of the liquid phase
γ	designates a property of the gas phase

REFERENCES

1. P. Henry, "Diffusion in Absorbing Media," *Proceedings of the Royal Society of London,* **171A,** 215–241 (1939).
2. J. Crank, *The Mathematics of Diffusion,* Oxford University Press, London, 354–367 (1975).
3. P. Nordon and H. G. David, *Int. J. of Heat and Mass Transfer,* **10,** 853–866 (1967).
4. B. Farnworth, *Textile Res. J.,* **56,** 653–665 (1986).
5. J. Wehner, B. Miller, and L. Rebenfeld, *Textile Res. J.* **58,** 581–592 (1988).
6. B. Jones, M. Ito, and E. McCullough, "Transient thermal response of clothing systems," *Proceedings of the International Conference on Environmental Ergonomics,* Austin, TX, October, 1990. pp. 66–67.
7. Y. Li and B. V. Holcombe, *Textile Res. J.,* **62,** 211–217 (1992).
8. C. Le and N. Ly, *Textile Res. J.,* **65**(4), 203–212, (1995).
9. D. Berger and C. Pei, *Int. J. of Heat and Mass Transfer,* **16,** 293–301 (1973).
10. E. R. G. Eckert and M. Faghri, *Int. J. of Heat and Mass Transfer,* **23,** 1613–1623 (1980).
11. M. Stanish, G. Schajer, and F. Kayihan, *AIChE J.,* **32,** 1301–1311, (1986).
12. A. V. Luikov, in *Advances in Heat Transfer,* T. F. Irvine, J. P. Hartnett, Eds., Academic Press, New York, 1964, Vol. 1, pp. 123–184.
13. S. Whitaker, in *Advances in Heat Transfer,* J. P. Hartnett, T. F. Irvine, Eds., Academic Press, New York, 1977, Vol. 13, pp. 119–200.
14. Y. Tao, R. Besant, and K. Rezkallah, *Int. J. of Heat and Mass Transfer,* **36,** 4433–4441, (1993).
15. P. Gibson and M. Charmchi, "A Numerical Model for Coupled Heat and Mass Transfer Through Hygroscopic Porous Textiles and Integration with a Human Thermal Physiology Control Model," presented at Fall 1995 General Technical Conference of The Fiber Society, Philadelphia, PA, November 13–15, 1995.
16. P. Gibson, C. Kendrick, D. Rivin, and M. Charmchi, "Application of Models for Coupled Heat and Mass Transfer Through Porous Media to Protective Clothing Systems for the Individual Soldier," *Proceedings 20th Army Science Conference,* Norfolk, VA, June 24–26, 1996.
17. P. Gibson and M. Charmchi, "Integration of a Human Thermal Physiology Control Model with a Numerical Model for Coupled Heat and Mass Transfer Through Hygroscopic Porous Textiles," Paper No. 96-WA/HT-29, 1996 International Mechanical Engineering Congress and Exposition, Atlanta, GA, November 17–22, 1996.
18. P. W. Gibson, *Governing Equations for Multiphase Heat and Mass Transfer in Hygroscopic Porous Media with Applications to Clothing Materials,* Technical Report Natick/TR-95/004, U.S. Army Natick Research, Development and Engineering Center, Natick, MA, November, 1994.
19. W. Lotens and G. Havenith, *Ergonomics,* **38**(6), 1092–1113, (1995).
20. E. Kerner, "The Electrical Conductivity of Composite Media," *Proceedings of the Physical Society,* **B69,** 802, (1956).
21. R. Progelhof, J. Throne, and R. Ruetsch, *Polym. Eng. and Sci.,* **16**(9), 615–625 (1976).
22. S. Morton and J. Hearle, *Physical Properties of Textile Fibres,* John Wiley and Sons, New York, 1975, pp. 586–591.

23. American Association of Textile Technology AATT Monograph No. 109, *Textile Fibers and Their Properties.*
24. P. W. Gibson, C. Kendrick, D. Rivin, L. Sicuranza, and M. Charmchi, *Journal of Coated Fabrics,* **24,** 322–345 (1995).
25. P. Gibson and M. Charmchi, "Convective and Diffusive Energy and Mass Transfer in Hygroscopic Porous Textile Materials," Paper No. 96-WA/HT-30, 1996 International Mechanical Engineering Congress and Exposition, Atlanta, Georgia, November 17–22, 1996.
26. Holman, J., *Heat Transfer,* McGraw-Hill, New York, 1990, p. 609.
27. W. Kays and M. Crawford, *Convective Heat and Mass Transfer,* McGraw-Hill, New York, 1993, pp. 125–140.
28. S. V. Patankar, *Numerical Heat Transfer and Fluid Flow,* Hemisphere Publishing, Washington, 1980, pp. 41–77.
29. F. Kreith and M. Bohn, *Principles of Heat Transfer,* Harper & Row Publishers, New York, 1986, pp. 496–497.